

## Equation of state of MgSiO<sub>3</sub> with the perovskite structure based on experimental measurement

SURENDRA K. SAXENA,<sup>1,\*</sup> LEONID S. DUBROVINSKY,<sup>1</sup> FARAMARZ TUTTI,<sup>1</sup>  
AND TRISTAN LE BIHAN<sup>2</sup>

<sup>1</sup>Department of Earth Sciences, Uppsala University, S-752 36 Uppsala, Sweden  
<sup>2</sup>European Synchrotron Radiation Facility, BP 220, 38043 Grenoble, Cedex, France

### ABSTRACT

We studied MgSiO<sub>3</sub> with the perovskite structure heated to temperatures up to 1500 K at pressures between 36 and 110 GPa with in-situ X-ray diffraction. The new pressure-volume-temperature (*P-V-T*) data were combined with literature data to provide thermal expansivity  $\alpha$  and compressibility  $\beta$  against  $T$  (in K):  $\alpha_T = 2.71 \times 10^{-5} + 1.80 \times 10^{-9} T - 1.48 T^2$  (Model 1) or  $\alpha_T = 2.13 \times 10^{-5} + 7.57 \times 10^{-9} T - 1.02 T^2$  (Model 2), and  $\beta_T = 3.735 \times 10^{-7} + 3.27 \times 10^{-11} T + 6.60 \times 10^{-15} T^2$ . Model 1 yields physical properties of perovskite that confirm Anderson's (1998) Debye approach; the model is valid for extrapolation to 3000 K or more. The parameters at 300 K are:  $\alpha = 1.1 \times 10^{-5}$ ,  $K_0$  (bulk modulus) = 261 GPa,  $K_0' = 4$  and  $(\partial K/\partial T)_P = -0.027$ . Thermal expansivity from this model does not fit the data of Funamori et al. (1996) at high temperature for  $P = 25$  GPa. Model 2 uses an equation for  $\alpha$  based on the data of Funamori et al. (1996), fits the available experimental data closely, and maintains conformity with Anderson's Debye approach. Heat capacity,  $C_p$ , data for perovskite is given by either:  $C_p = 110.8 + 8.031 \times 10^{-3} T - 1.302 \times 10^{-7} T^2 - 1.647 \times 10^7 T^2 + 2.755 \times 10^9 T^{-3} + 267.5 T^{-0.5} + 9287 T^{-1}$  (Model 1) or  $C_p = 121.33 + 2.77 \times 10^{-3} T - 2.585 \times 10^{-6} T^2 - 1.710 \times 10^7 T + 2.792 \times 10^9 T^{-3} - 169 T^{-0.5} + 15782 T^{-1}$  (Model 2).

### INTRODUCTION

Perovskite (MgSiO<sub>3</sub>) is considered to be an important phase in Earth's mantle. This is reflected in the number of several recent papers on this topic (Mao et al. 1991; Wang et al. 1994; Morishima et al. 1994; Utsumi et al. 1995; Fiquet et al. 1998; Anderson 1998; Funamori et al. 1996). Fiquet et al. (1998) reviewed the previous experimental studies and concluded a definite need existed for in-situ *P-V-T* data on perovskite at deep mantle pressures. They extended the pressure range to 57 GPa by several GPa over that of Funamori et al. (1996) and heated samples up to temperatures of 2668 K. In the present study, pressures up to 110 GPa and temperatures close to 1500 K were reached. The goal was to obtain a complete set of physical parameters for perovskite.

### EXPERIMENTAL TECHNIQUE

The external electric heater for diamond-anvil cell that was used in this study had two Re or Mo gaskets in which holes were drilled large enough to allow the diamond anvils pass to nearly one third of their height (Fig. 1). Electric leads were attached and the current passed through graphite foils between which the sample holding gasket was sandwiched. A micro thermocouple (PH type B) was attached to the sample gasket diamond interface.

An Re gasket with a 50  $\mu\text{m}$  hole was used here. This design had the advantage that the entire sample chamber including significant parts of the diamonds were surrounded by the graphite heater and heated uniformly. For the safety of the diamonds, Ar with 1% H<sub>2</sub> was continuously passed through the piston-cylinder assembly of the cell. In-situ melting temperature for indium and tin using this method could be determined with an accuracy of 7 °C at a pressure of 15 GPa (Rekhi et al. 1998).

The starting material was natural enstatite (Stakholmen, Hälsingland, Sweden) with less than 1% aluminum and iron obtained from U. Hålenius, Riksmuseet, Stockholm. It was mixed with a small piece of platinum, compressed into a thin disk, and placed in the 50  $\mu\text{m}$  hole in the rhenium gasket. The sample was studied at ESRF, Grenoble, with in-situ X-ray diffraction. The diffraction studies were carried out using monochromatic radiation ( $\lambda = 0.3738 \text{ \AA}$ ). X-rays were focused to a spot of 10  $\mu\text{m}$  in diameter on the sample. The data (e.g., Fig. 2) were collected from 4 to 25 °  $\theta$  using imaging plate employing the fast-scan technique developed at ESRF. The pressure at room temperature as well as at higher temperatures was obtained from the equation of state of platinum (Jamieson et al. 1982), and the temperature was measured directly from the type B micro-thermocouple. The power was increased in small increments and X-ray data was collected at each temperature for 1 to 3 min.

\* E-mail: surendra.saxena@geo.uu.se

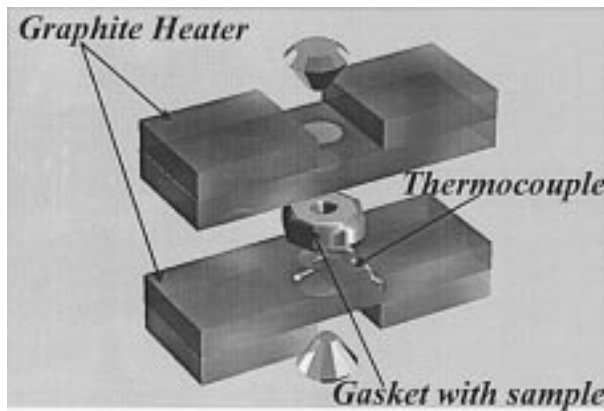


FIGURE 1. The high-temperature cell assembly using graphite foils. See text for description.

## RESULTS

Table 1 shows the pressure-volume-temperature data as measured in this work. Because the sample is uniformly heated, temperature gradient in the sample is not a significant factor (Rekhi et al. 1998; Dubrovinsky et al. 1998). The studies of Meng et al. (1993) and Fiquet et al. (1998) have shown that the effect of differential stress is minimal at high temperatures. One former study (Dubrovinsky et al. 1998) established that differential stress decreases from  $\sim 1.5$  GPa at 600 K to  $\sim 0.25$  GPa at 850 K.

## ANALYSIS AND DISCUSSION

### Thermodynamics

Saxena et al. (1993) demonstrated the importance of relating the physical (thermal expansion and compressibility) and thermochemical (heat capacity) parameters and showed their internal consistency when extrapolating data;  $C_p$  is given by:

$$C_p = C_v + \alpha^2 V K_T T$$

+ other anharmonic and ordering contributions (1)

where  $V$  is the molar volume.

Polynomial expressions in  $T$  have been used for fitting  $\alpha$  and  $K$  to experimental data:

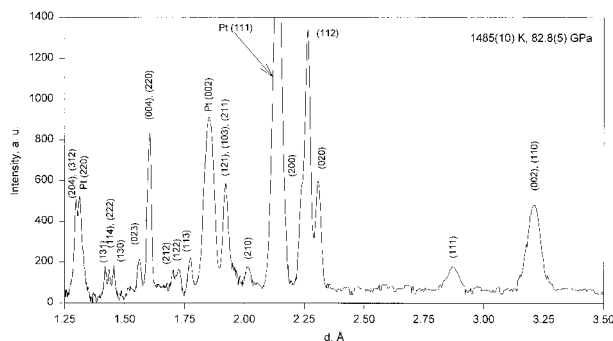


FIGURE 2. X-ray diffraction pattern of a heated perovskite.

TABLE 1. Measured volume data on  $\text{MgSiO}_3$  perovskite

$P^*$ (GPa)	$T^\dagger$ (K)	$V$ ( $\text{cm}^3/\text{mol}$ )
36.2	300	21.874 (11)
53.8	300	20.995 (12)
60.1	300	20.717 (9)
65.5	300	20.491 (11)
67.5	300	20.410 (10)
73.3	747	20.257 (8)
74.3	685	20.203 (13)
75.8	1138	20.262 (9)
77.6	300	20.022 (8)
78.0	805	20.090 (12)
78.4	1087	20.148 (13)
78.6	300	19.986 (11)
78.7	1022	20.120 (12)
79.5	915	20.063 (11)
79.7	947	20.063 (14)
79.9	747	20.000 (10)
80.1	300	19.93 (9)
81.1	1180	20.069 (9)
81.3	585	19.920 (11)
81.5	1280	20.082 (10)
81.8	1140	20.034 (12)
82.2	300	19.857 (11)
82.5	300	19.846 (14)
82.8	1485	20.09 (10)
84.1	655	19.834 (11)
84.9	917	19.865 (12)
87.4	1170	19.839 (12)
91.9	1245	19.700 (10)
92.5	1087	19.562 (11)
94.3	1357	19.646 (12)
94.4	1357	19.643 (10)
97.7	1255	19.506 (13)
101.4	1170	19.368 (14)
104.2	1170	19.279 (12)
107.3	1357	19.226 (14)
108.9	747	19.047 (13)
109.1	1357	19.172 (15)

\* Pressure determined from Pt equation of state. Points with error 0.5 GPa were rejected.

† Temperature errors as measured by thermocouple are less than  $\pm 10^\circ$  K.

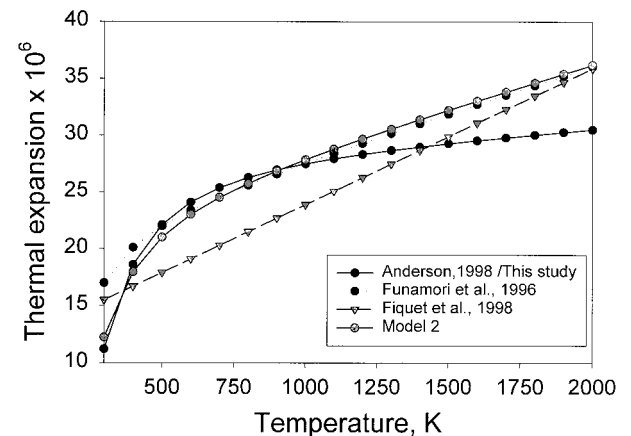
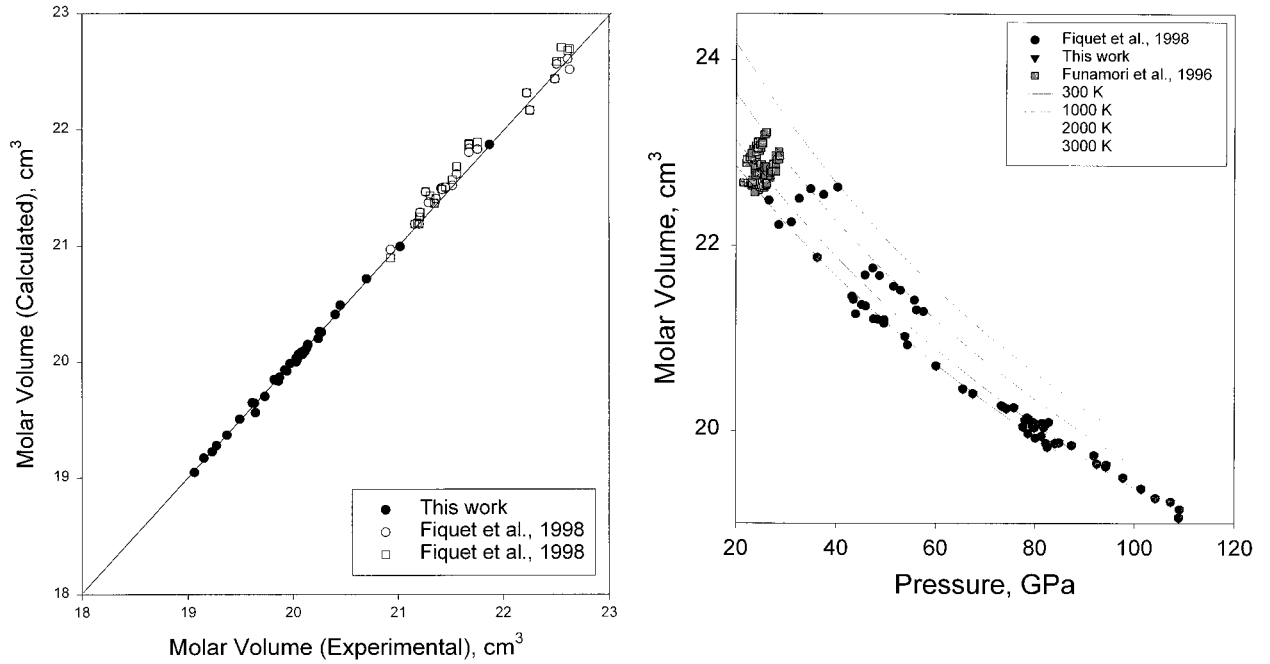


FIGURE 3. Data on thermal expansion of perovskite at 1 atm. Model 1 data are essentially as chosen by Anderson (1988). Model 2 data are generated by taking into consideration the thermal expansivity of Funamori et al. (1996).



**FIGURE 4.** (left) Experimental data on molar volume from this study and from Fiquet et al. (1998) plotted against the calculated data using Model 1 (Eqs. 14 and 17) and Model 2 (Eqs. 20 and 17). The present data fit both the model with same precision (Model 2 points not shown). Similarly the data of Fiquet et al. (1998) fit both the models quite well. The data cover the pressure range of 0 to 105 GPa at temperatures up to 3000 K. (right) Three sets of experimental data are plotted to show the variation of molar volume with pressure and temperature. The curves are calculated using Model 1.

**TABLE 2.** Data calculated using Model 1

$T$ K	$C_p$ J/mol	$K_T$ GPa	$\gamma_{th}$	$V(\text{mol})$ $\text{cm}^3$	$\alpha$ $10^{-6}/\text{K}$	$C_v$ J/mol	$K_s$ GPa	$\delta_T$	$\alpha K_T$ MPa
300.00	78.68	260.51	0.89	24.45	1.12	78.44	261.26	9.26	2.92
400.00	90.71	258.00	1.27	24.49	1.86	89.84	260.49	5.64	4.79
500.00	101.49	255.45	1.37	24.54	2.21	99.95	259.30	4.79	5.64
600.00	108.98	252.87	1.40	24.59	2.41	106.80	257.97	4.44	6.09
700.00	114.16	250.25	1.41	24.65	2.53	111.36	256.43	4.26	6.34
800.00	117.86	247.61	1.41	24.72	2.62	114.45	254.88	4.16	6.49
900.00	120.60	244.95	1.41	24.78	2.69	116.61	253.34	4.10	6.59
1000.00	122.73	242.26	1.40	24.85	2.74	118.16	251.42	4.06	6.64
1100.00	124.44	239.56	1.40	24.92	2.79	119.29	249.89	4.05	6.67
1200.00	125.87	236.84	1.40	24.99	2.82	120.14	247.90	4.04	6.69
1300.00	127.09	234.11	1.39	25.06	2.86	120.80	246.38	4.04	6.69
1400.00	128.17	231.38	1.39	25.13	2.89	121.31	244.34	4.04	6.68
1500.00	129.14	228.63	1.38	25.21	2.91	121.72	242.36	4.05	6.66
1600.00	130.04	225.89	1.38	25.28	2.94	122.06	240.25	4.07	6.64
1700.00	130.88	223.14	1.38	25.35	2.96	122.33	238.73	4.08	6.62
1800.00	131.68	220.39	1.37	25.43	2.99	122.57	236.58	4.10	6.59
1900.00	132.45	217.65	1.37	25.51	3.01	122.78	234.53	4.12	6.55
2000.00	133.19	214.92	1.36	25.58	3.03	122.96	232.46	4.14	6.52
2100.00	133.91	212.19	1.36	25.66	3.05	123.12	230.84	4.17	6.48
2200.00	134.61	209.48	1.36	25.74	3.08	123.27	228.76	4.19	6.44
2300.00	135.31	206.77	1.36	25.82	3.10	123.40	226.67	4.22	6.40
2400.00	135.99	204.08	1.35	25.90	3.12	123.53	224.43	4.25	6.36
2500.00	136.66	201.41	1.35	25.98	3.14	123.65	222.32	4.27	6.32
2600.00	137.33	198.75	1.35	26.06	3.16	123.77	220.74	4.30	6.27
2700.00	138.00	196.11	1.34	26.15	3.18	123.88	218.65	4.34	6.23
2800.00	138.66	193.49	1.34	26.23	3.20	123.99	216.55	4.37	6.18
2900.00	139.31	190.89	1.33	26.31	3.21	124.10	214.28	4.40	6.14
3000.00	139.97	188.32	1.33	26.40	3.23	124.21	212.18	4.43	6.09

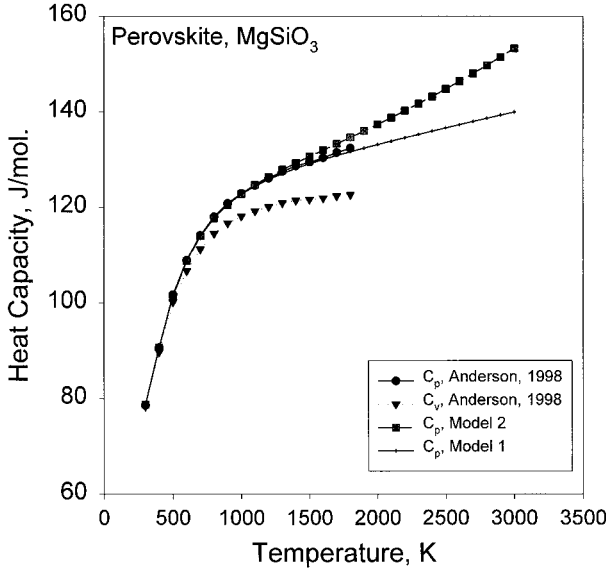


**FIGURE 5.** Heat capacity data plotted as a function of temperature.  $C_p$  calculated from Model 1 differs from that calculated by Model 2 because of different  $\alpha_T$  data of Funamori et al. (1996). The  $C_v$  is for a Debye-like solid as calculated by Anderson (1998). The  $\alpha^2 VKT$  terms are from Equations 17 and 14 for Model 1 and from Equations 17 and 20 for Model 2.

$$\alpha = a + bT + cT^{-2} \quad (2)$$

$$K = K_0 + K_1T + \dots \quad (3)$$

The use of polynomial expressions and their pitfalls has been discussed by Saxena et al. (1993) where a description of obtaining internally consistent data can also be found.

For bulk modulus, extrapolation of the data in optimizing the  $C_p$  and  $C_v$  relationship yields better fits if compressibility is used instead (Saxena et al. 1993).

$$\beta = \beta_0 + \beta_1T + \beta_2T^2 + \dots \quad (4)$$

The Birch-Murnahan (B-M) equation of state is given by

$$P_{B-M} = \frac{3}{2}K_{T,0} \left[ \left( \frac{V_0}{V} \right)^{7/3} - \left( \frac{V_0}{V} \right)^{5/3} \right] \times \left\{ 1 - \frac{3}{4}(4 - K'_{T,0}) \left[ \left( \frac{V_0}{V} \right)^{2/3} - 1 \right] + \dots \right\} \quad (5)$$

where  $K_{T,0}$  and  $K'_{T,0}$  ( $=[\delta K_{T,0}/\delta P]_T$ ) are the isothermal bulk modulus and its pressure derivative at 298 K, respectively. (The zero will be dropped from the subscript in the labels and instead stipulated that  $K_T$  and  $K'_T$  are values at 0 pressure).

Because all the information available on the temperature dependence of  $\alpha_T$  and  $K_T$ , the isothermal form of the B-M equation of state (see Saxena and Zhang 1989) at different temperatures can be applied predictably as follows.

$VdP$  was calculated by adopting the third-order B-M equation of state (Eq. 5) where the temperature depen-

dence of the isothermal bulk modulus was included and  $V^0/V$  was replaced by  $V(1,T)/V(P,T)$ . The temperature dependence of all variables, except of the pressure derivative  $K'_T$  was known from the data systematization (Anderson 1998; Fiquet et al. 1998; Funamori et al. 1996). By using the experimental data on in-situ  $P$ - $V$ - $T$  determinations, the temperature dependence of the pressure derivative  $K'_p$  may be determined by expressing  $(\delta K'_T/\delta P)_T$  with an appropriate function, e.g.,

$$(\delta K'_T/dP)_T = K'_{300} + K_4(T - 300)\ln(T/300) \quad (6)$$

where  $K'_{300}$  is the pressure derivative in the B-M equation and  $K_4$  the temperature coefficient (not to be confused with  $K''$  the second derivative of the bulk modulus). Saxena et al. (1993) called this model the high-temperature Birch-Murnahan (HTB-M) model. For convenience,  $PdV$  may be calculated from Equation 7 instead of from  $VdP$ . The relation between  $PdV$  and  $VdP$  is given by

$$\int_1^P V dP = \int_{V(P,T)}^{V(1,T)} P dV + V(P-1) \quad (7)$$

where

$$\int_{V(P,T)}^{V(1,T)} P dV = \frac{3}{2}K_T V(1,T) \left[ \frac{3}{4}(1+2x)(Y^{4/3}-1) - \frac{3}{2}(1+x)(Y^{2/3}-1) - \frac{1}{2}x(Y^2-1) \right] \quad (8)$$

and

$$x = \frac{3}{4} \left[ 4 - \left( \frac{\partial K_T}{\partial P} \right)_T \right] \quad \text{and} \quad Y = \frac{V(1,T)}{V(P,T)}. \quad (9)$$

Equation 7 is sufficient to determine the pressure part of the Gibbs energy of any phase (within the range of pressure of the applicability of the equation of state); however, due to assumptions involved in the  $C_p/C_v$  optimization (e.g., empirical polynomial forms and/or Kieffer's model of  $C_v$ ), it is necessary to calculate certain characteristic parameters as used in other  $P$ - $V$ - $T$  models (e.g., Anderson 1995; Jeanloz and Knittle 1986) and compare the data with theory based data (Anderson 1998). One such parameter is the Grüneisen parameter  $\gamma = \alpha_T K_T V/C_v$  and its functional dependence on temperature. The latter information is useful in deciding the applicability of the Mie-Grüneisen equation. The Anderson-Grüneisen constant ( $\delta$ ) given by:

$$\delta_T = -(1/\alpha K_T)(dK_T/dT)_p \quad (10)$$

is presented here to facilitate comparison of the data with those calculated using Anderson's model.

Here,  $C_p$  is formulated by taking into account the important role of the  $\alpha_T^2 VK_T T$  term, which links the measured heat capacity with the measured physical properties of solids at high temperature. This provides an additional

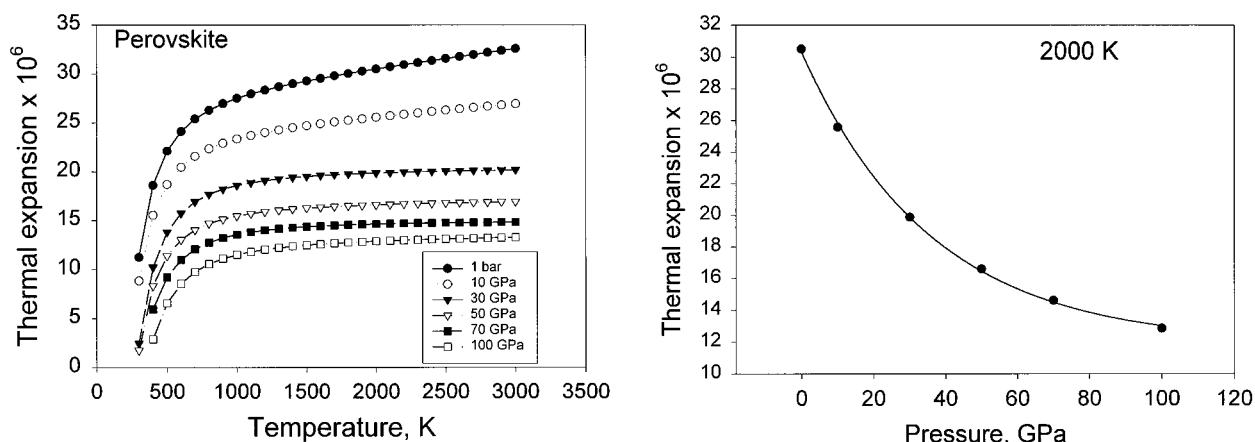


FIGURE 6. (left) Variation of  $\alpha_T$  as a function of pressure calculated with Model 1. (right) Effect of pressure on  $\alpha_T$  at 2000 K. The figures show that with increasing pressure and temperature,  $\alpha$  approaches a constant value.

constraint for evaluating an internally consistent thermochemical and thermophysical data set based on data from the calorimetric measurements, from the experimental phase equilibria and from the measurements of physical properties.

The assessed  $C_p$  data are presented with a flexible  $C_p$  formulation adopted at many centers (e.g., A.D. Pelton with the F\*A\*C\*T system at Ecole Polytechnique, Montreal; B. Sundman with THERMOCALC at the Royal Technical University at Stockholm) working with large databases. The formulation is:

$$C_p = a + bT + cT^{-2} + dT^2 + eT^3 + fT^{-0.5} + gT^{-1}. \quad (11)$$

#### Data based on experiments

Bina (1995) discussed the equation of state data for perovskite and made a detailed study of uncertainties and mutual inconsistencies in the available experimental data. Fiquet et al. (1998) presented new experimental data and also reviewed the existing data (e.g., Mao et al. 1991; Wang et al. 1991, 1994; Funamori and Yagi 1993; Funamori et al. 1996; Morishima et al. 1994; Utsumi et al. 1995). Their physical data on perovskite are fitted by the following equations:

$$\alpha_T = (1.19 \pm 0.17) \times 10^{-5} + (1.20 \pm 0.10) \times 10^{-8} T \quad (12)$$

$$K_T (\text{in GPa}) = 261 - 0.027 T. \quad (13)$$

These equations are consistent with previous experimental data within mutual error limits. Funamori et al. (1996) carefully analyzed their data collected between pressures of 21 to 29 GPa and temperatures of 300 to 2000 K. Their thermal expansivity at 25 GPa pressure must be considered reliable.

#### Anderson's Debye approach

Anderson (1998) proposed that perovskite is a Debye-like mineral. He showed this by calculating specific heat,  $C_v$ , of MgO using the Debye model and comparing the

calculated  $C_p$  with the experimental data. He argued that the density of states of perovskite is similar to that of MgO. He demonstrated convincingly that the limited heat capacity  $C_p$  data available on perovskite can be matched by choosing the appropriate data on  $\alpha_T$  and  $K_T$  and the Debye  $C_v$ . Anderson's data fitted on  $\alpha$  becomes the following equation:

$$\alpha_T = 2.71 \times 10^{-5} + 1.80 \times 10^{-9} T - 1.48 T^{-2}. \quad (14)$$

Anderson (1998) chose his  $\alpha$  data at low temperatures from Funamori et al. (1996) but the high-temperature data differ significantly (Fig. 3). For bulk modulus, Anderson (1998) used the data of Jackson and Ridgen (1996) and Yeganeh-Haeri (1994). His data on bulk modulus as a function of temperature can be fitted by the equation:

$$K_T = 264.4 \times 10^4 - 0.026 T \quad (15)$$

Additionally, he determined the temperature dependence of  $K'_0$  as

$$K'_T = K'_{300} + 1.4 \times 10^{-4}(T-300) \quad (16)$$

#### Internally consistent perovskite thermodynamic data

This study demonstrates that the experimental results of Fiquet et al. (1998), which accounts for the previous experimental data, is quite similar to Anderson's Debye-like model for perovskite. Using the previously adopted approach (Saxena et al. 1993) of compressibility expression for extrapolation, the equations for the two data sets are:

$$\beta = 3.735 \times 10^{-7} + 3.27 \times 10^{-11} T + 6.60 \times 10^{-15} T^2 \quad (17)$$

(data of Fiquet et al. 1998)

$$\beta = 3.705 \times 10^{-7} + 3.10 \times 10^{-11} T + 6.86 \times 10^{-15} T^2. \quad (18)$$

(data of Anderson 1998)

The coefficients in the two equations are quite comparable.

A fit of the combined data sets of Fiquet et al. (1998)

TABLE 3. Data calculated using Model 2

$T$ K	$C_p$ J/mol	$K_T$ GPa	$\gamma_{Th}$	$V(\text{mol})$ $\text{cm}^3$	$10^{-6}/K$	$C_v$ J/mol	$K_s$ GPa	$\delta_T$	$\alpha K_T$ MPa
300.00	78.72	260.51	0.99	24.45	1.22	78.44	260.81	8.46	3.19
400.00	90.65	258.00	1.26	24.49	1.80	89.84	258.86	5.83	4.63
500.00	101.33	255.45	1.32	24.53	2.10	99.95	256.89	5.03	5.37
600.00	108.78	252.87	1.34	24.59	2.30	106.80	254.90	4.64	5.82
700.00	113.95	250.25	1.36	24.65	2.45	111.36	252.89	4.40	6.14
800.00	117.70	247.61	1.38	24.71	2.58	114.45	250.87	4.23	6.38
900.00	120.55	244.95	1.40	24.77	2.69	116.61	248.85	4.10	6.58
1000.00	122.83	242.26	1.42	24.84	2.79	118.16	246.82	4.00	6.75
1100.00	124.73	239.56	1.44	24.91	2.88	119.29	244.79	3.91	6.90
1200.00	126.40	236.84	1.46	24.98	2.97	120.14	242.77	3.84	7.03
1300.00	127.91	234.11	1.48	25.06	3.05	120.80	240.76	3.78	7.15
1400.00	129.33	231.38	1.51	25.14	3.14	121.31	238.76	3.72	7.26
1500.00	130.69	228.63	1.53	25.22	3.22	121.72	236.77	3.67	7.36
1600.00	132.03	225.89	1.55	25.30	3.30	122.06	234.79	3.62	7.46
1700.00	133.35	223.14	1.57	25.39	3.38	122.33	232.82	3.58	7.55
1800.00	134.68	220.39	1.59	25.47	3.46	122.57	230.87	3.54	7.63
1900.00	136.03	217.65	1.60	25.56	3.54	122.78	228.94	3.50	7.71
2000.00	137.40	214.92	1.62	25.65	3.62	122.96	227.02	3.47	7.78
2100.00	138.80	212.19	1.64	25.75	3.70	123.12	225.12	3.44	7.85
2200.00	140.24	209.48	1.66	25.84	3.78	123.27	223.24	3.41	7.91
2300.00	141.72	206.77	1.67	25.94	3.85	123.40	221.37	3.39	7.97
2400.00	143.23	204.08	1.69	26.04	3.93	123.53	219.52	3.37	8.02
2500.00	144.79	201.41	1.71	26.15	4.01	123.65	217.69	3.35	8.07
2600.00	146.40	198.75	1.72	26.25	4.08	123.77	215.88	3.33	8.12
2700.00	148.05	196.11	1.74	26.36	4.16	123.88	214.09	3.31	8.16
2800.00	149.75	193.49	1.75	26.47	4.24	123.99	212.32	3.29	8.20
2900.00	151.49	190.89	1.76	26.59	4.31	124.10	210.56	3.28	8.24
3000.00	153.29	188.32	1.78	26.70	4.39	124.21	208.83	3.27	8.27

at 300 K and this study using Equation 5 led to closely similar parameters for compressibility as obtained by Fiquet et al. (1998). However, the choice of thermal expansivity is difficult. From Figure 3,  $\alpha_T$  of Funamori et al. (1996) differs enough from that of Anderson's adopted data to require consideration of two expressions for  $\alpha_T$ :

$$\alpha_T = 2.71 \times 10^{-5} + 1.80 \times 10^{-9} T - 1.48 T^{-2}$$

(fitted to Anderson's data 1998) (19)

and

$$\alpha_T = 2.13 \times 10^{-5} + 7.57 \times 10^{-9} T - 1.02 T^{-2}$$

(fitted to Funamori et al. 1996) (20)

Equation 20 fits the experimental data quite well (Fig. 3). Figure 4 (left) shows a comparison of the calculated with the experimental data of this study and of Fiquet et al. (1998). Equation 14 reproduces the thermal expansivity adopted by Anderson (1998). The equation of state gives the same level of accuracy of fit to experimental data of Fiquet et al. (1998). Figure 4 (left and right) show a general consistency of the pressure-volume-temperature data with the modeled data. Two equations of state have been created because of the differences in the choice of thermal expansivity. The first model employs Equations 14 and 17 and matches Anderson's data in all respects. The second model uses Equations 20 and 17.

### Heat capacity at high temperatures

Because the available experimental pressure-volume-temperature data covers a broad temperature range, the

term  $\alpha^2 VKT$  (cf. Eq. 1) can be calculated to temperatures as high as 3000 K without significant extrapolation. Therefore, it is possible to calculate  $C_p$  and other geophysically important data using the results presented here.

Table 2 shows the calculated data on  $C_p$ ,  $C_v$ ,  $\alpha$ ,  $K_T$ ,  $K_s$  (adiabatic bulk modulus),  $\gamma_{Th}$ , and  $\delta_T$  at 1 atm. Extrapolation was done using a polynomial in temperature for  $C_v$  (Anderson's Debye-like solid) and for  $\alpha_T$  and  $K_T$  (or compressibility). Heat capacity at constant pressure was then calculated using Equation 1. The resulting data on  $C_p$  and  $C_v$  are displayed in Figure 5. Figure 6 (left) shows  $\alpha_T$  as a function of pressure, which is calculated by fitting isobaric  $V(T)$  data as a function of temperature. The temperature dependence of  $\alpha_T$  became negligible  $\sim 1000$  K at pressures  $> 30$  GPa. The pressure dependence of thermal expansion also decreased with pressure and approached a constant value at pressures above 100 GPa (Fig. 6 right).

Figure 6 shows use of the  $\alpha_T$  data of Funamori et al. (1996) to 2000 K as extrapolated to 3000 K with the same equation, thus obtaining higher heat capacity values. Figure 7 shows the finally evaluated data on molar volume at 25 GPa pressure by Funamori et al. (1996). The molar volumes calculated with Model 1 are close to about 1400 K. Although the Model 1 volumes at high temperatures lie within the error of the experimental data, the difference was sufficient to cause a change in thermal expansivity and in the data on heat capacity as displayed in Figures 2 and 4. The difference in  $C_p$  data could be large enough to affect the calculations on the thermodynamic stability of perovskite. Therefore, it is important to con-

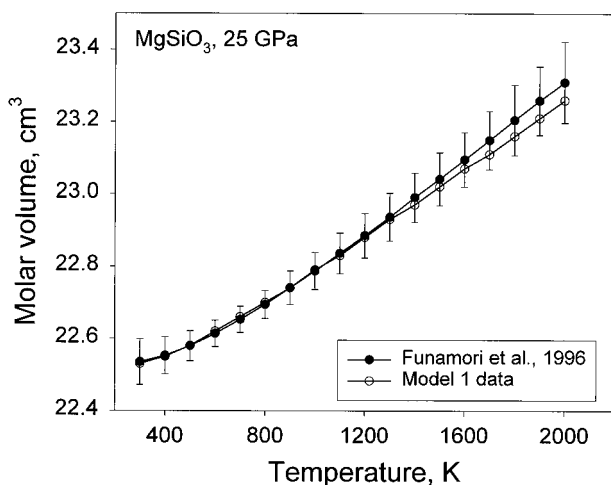


FIGURE 7. High-temperature molar volume data at a pressure of 25 GPa. The difference at high temperature between the data calculated with Model 1 and the data of Funamori et al. (1996) is significant enough to change  $C_p$  data substantially at high temperatures (Fig. 4, Table 2).

sider the data (Table 3) based on Model 2 (Eq. 17 for  $\beta$  and Eq. 20 for  $\alpha$ ).

### CONCLUSIONS

The available data on pressure-volume-temperature of perovskite can be fitted with equations for compressibility and thermal expansion, which confirm the validity of Anderson's (1998) Debye-like solid model. The data attest that the thermodynamic Grüneisen parameter (Table 2 or Table 3) approaches a constant value. Similarly, the Anderson-Grüneisen parameter approaches a stable value.

As amplified by Anderson (1998), the precision in determining  $\alpha_T$  is critical in calculating heat capacity  $C_p$  using the Debye  $C_v$ . For perovskite, the situation is well resolved to temperatures as high as 1800 K. The slightly higher  $\alpha_T$  values at higher temperatures by Funamori et al. (1996) lead to certain differences in thermodynamic data, which may be significant in phase equilibrium calculations. Until this issue is resolved, the heat capacity and other data within the limits imposed by the two models must be considered.

### ACKNOWLEDGMENTS

We thank D. Häusermann and M. Mezouar for their help at ESRF and the Swedish Science Research Foundation for support. In revising the paper, we benefitted from the advice of Craig Bina and an anonymous reviewer.

### REFERENCES CITED

Akaogi, M. and Ito, E. (1993) Refinement of enthalpy measurement of  $\text{MgSiO}_3$  perovskite and negative pressure-temperature slopes for perovskite-forming reactions. *Geophysical Research Letters*, 20, 1839–1842.  
 ——— (1995) Equations of state of solids for geophysics and ceramic science, 405 p. Oxford University Press, Oxford, New York.

Anderson, O.L. (1998) Thermoelastic properties of  $\text{MgSiO}_3$  perovskite using the Debye approach. *American Mineralogist*, 83, 23–25.  
 Dubrovinsky, L.S., Saxena, S.K., and Lazor, P. (1998) Stability of  $\beta$ -iron: a new synchrotron X-ray study of heated iron at high pressure. *European Journal of Mineralogy*, 10, 43–47.  
 Fiquet, G., Andrault, D., Dewaele, A., Charpin, T., Kunz, M., and Häusermann, D. (1998)  $P$ - $V$ - $T$  equation of state of  $\text{MgSiO}_3$  perovskite. *Physics of Earth and Planetary Interiors*, 105, 21–31.  
 Funamori, N. and Yagi, T. (1993) High pressure and high temperature in situ X-ray observation of  $\text{MgSiO}_3$  perovskite under lower mantle condition. *Geophysical Research Letters*, 20, 387–390.  
 Funamori, N., Yagi, T., Utsumi, W., Kondo, T., Uchida, T., and Funamori, M. (1996) Thermoelastic properties of  $\text{MgSiO}_3$  perovskite determined by in situ X-ray observations up to 30 GPa and 2000 K. *Journal of Geophysical Research*, 101, 8257–8269.  
 Jackson, I. and Rigden, S. (1996) Analysis of  $P$ - $V$ - $T$  data: constraints on the thermoelastic properties of high-pressure minerals. *Physics of the Earth and Planetary Interiors*, 96, 85–112.  
 Jamieson, J.C., Fritz, J.N., and Manghnani, M.H. (1982) Pressure measurement at high temperature in X-ray diffraction studies: gold as a primary standard. In S. Akimoto and M.H. Manghnani, Eds., *High Pressure Research in Geophysics*, p. 27–48. Reidel, Boston.  
 Jeanloz, R. and Knittle, E. (1986) Reduction of mantle and core properties to a standard state by adiabatic decompression. In S.K. Saxena, Ed., *Chemistry and Physics of Terrestrial Planets*, p. 275–309. Springer-Verlag, New York.  
 Mao, H.K., Hemley, R.J., Fei, Y., Shu, J.F., Chen, L.C., Jephcoat, A.P., Wu, Y., and Bassett, W.A. (1991) Effect of pressure, temperature and composition of lattice parameters and density of  $(\text{Fe,Mg})\text{SiO}_3$ -perovskite to 30 GPa. *Journal of Geophysical Research*, 69, 8069–8079.  
 Meng, Y., Weidner, D.J., and Fei, Y. (1993) Deviatoric stress in a quasi-hydrostatic diamond-anvil cell: effect on the volume-based pressure calibration. *Geophysical Research Letters*, 20, 1147–1150.  
 Morishima, H., Ohtani, E., Kato, T., Shimomura, O., and Kikegawa, T. (1994) Thermal expansion of  $\text{MgSiO}_3$  perovskite at 20.5 GPa. *Geophysical Research Letters*, 21, 899–902.  
 Rekhii, S. and Dubrovinsky, L.S. (1998) Pressure-temperature calibration of Sm-YAG and ruby fluorescence. *High Pressure-High Temperature* (submitted).  
 Saxena, S.K. (1996) Earth mineralogical model: Gibbs free energy minimization computation in the system  $\text{MgO-FeO-SiO}_2$ . *Geochimica et Cosmochimica Acta*, 60, 2379–2395.  
 Saxena, S.K. and Zhang, J. (1989) Assessed high-temperature thermochemical data on some solids. *Journal of Physics and Chemistry of Solids*, 50, 723–727.  
 Saxena, S.K., Chatterjee, N., Fei, Y., and Shen, G. (1993) *An Assessment of Thermodynamics of Oxides and Silicates*, 250 pp. Springer-Verlag, New York.  
 Utsumi, W., Funamori, N., Yagi, T., Ito, E., Kikegawa, T., and Shimomura, O. (1995) Thermal expansivity of  $\text{MgSiO}_3$  perovskite under high pressures up to 20 GPa. *Geophysical Research Letters*, 22, 1005–1008.  
 Wang, Y., Weidner, D.J., Liebermann, R.C., Lui, X., Ko, J., Vaughan, M.T., Zhao, Y., Yeganeh-Haeri, A., and Pacalo, R.E.G. (1991) Phase transformation and thermal expansion of  $\text{MgSiO}_3$  perovskite. *Science*, 251, 410–413.  
 Wang, Y., Weidner, D.J., Liebermann, R.C., and Zhao, Y. (1994)  $PVT$  equation of state of  $(\text{Mg, Fe})\text{SiO}_3$  perovskite: constraints on composition of the lower mantle. *Physics of Earth and Planetary Interiors*, 83, 13–40.  
 Yeganeh-Haeri, A. (1994) Synthesis and re-investigation of the elastic properties of single-crystal magnesium silicate perovskite. *Physics of the Earth and Planetary Interiors*, 87, 111–112.  
 Yeganeh-Haeri, A., Weidner, D.J., and Ito, E. (1989) Elasticity of  $\text{MgSiO}_3$  in the perovskite structure. *Science*, 243, 787–789.

MANUSCRIPT RECEIVED OCTOBER 5, 1998

MANUSCRIPT ACCEPTED OCTOBER 2, 1998

PAPER HANDLED BY ROBERT M. HAZEN